

## Carbon Fibers Derived from UV-Assisted Stabilization of Wet-Spun Polyacrylonitrile Fibers

Marlon S. Morales,<sup>1,2</sup> Amod A. Ogale<sup>1,2</sup>

<sup>1</sup>Department of Chemical Engineering, Earle Hall, Clemson University, Clemson, South Carolina 29634-0910

<sup>2</sup>Center for Advanced Engineering Fibers and Films, Earle Hall, Clemson University, Clemson, South Carolina 29634-0910

Correspondence to: A. A. Ogale (E-mail: ogale@clemson.edu)

**ABSTRACT:** A rapid, dual-stabilization route for the production of carbon fibers from polyacrylonitrile (PAN) precursor fibers is reported. A photoinitiator, 4,4'-bis(diethylamino)benzophenone, was added to PAN solution before the fiber wet-spinning step. After a short UV treatment that induced cyclization and crosslinking at a lower temperature, precursor fibers could be rapidly thermo-oxidatively stabilized and successfully carbonized. Scanning electron microscopy micrographs show no deterioration of the microstructure or hollow-core formation in the fibers due to UV treatment or presence of photoinitiator. Fast-thermally stabilized pure PAN-based carbon fibers show hollow-core fiber defects due to inadequate thermal stabilization, but such defects were not observed in carbon fibers derived from fast-thermally stabilized fibers that contained photoinitiator and were UV treated. Tensile testing results confirm that fibers containing 1 wt % photoinitiator and UV treated for 5 min display higher tensile modulus than all other sets of thermally stabilized and carbonized fibers. Wide-angle X-ray diffraction results show a higher development of the aromatic structure and molecular orientation in thermally stabilized fibers. No significant increase in interplanar spacing or decrease in crystals size were observed within the UV-stabilized carbon fibers containing photoinitiator, but such fibers retain a higher extent of molecular orientation when compared with control fibers. These results establish for the first time, the positive effect of the external addition of photoinitiator and UV treatment on the properties of the PAN-based fibers, and may be used to reduce the precursor stabilization time for faster carbon fiber production rate. © 2014 Wiley Periodicals, Inc. *J. Appl. Polym. Sci.* **2014**, *131*, 40623.

**KEYWORDS:** crosslinking; fibers; mechanical properties; morphology; X-ray

Received 27 December 2013; accepted 16 February 2014

DOI: 10.1002/app.40623

### INTRODUCTION

High-strength carbon fibers used in structural composites for aerospace applications are derived from solution-spun polyacrylonitrile (PAN) precursor fibers.<sup>1–3</sup> However, the higher cost of carbon fibers, as compared with that of other reinforcing materials (viz., glass fibers), limits their use for the high-end applications where strength-to-density ratio is critical.<sup>2–5</sup> The demand for carbon fibers is expected to grow to about 150,000 t over the next decade from current demand of 40,000 t. However, a large fraction of the increase is anticipated in the industrial sector that is cost sensitive.<sup>6</sup> For cost-effective products, such as automotive application, there is a need for the development of novel processes and precursors to reduce the carbon fiber production cost and expand the use of carbon fibers.

For the conversion of PAN into carbon fibers, thermal oxidative stabilization and carbonization steps have to be conducted.<sup>2,7,8</sup> The thermal stabilization process is believed to be the most important step during the carbon fiber manufacture, because

the conditions used during stabilization lead to most of the final carbon fiber properties.<sup>9,10</sup> Also, thermal stabilization is the rate-limiting step in the production of PAN-based carbon fibers.<sup>1,11</sup> During thermo-oxidative stabilization, heat is produced by exothermic reactions and a temperature gradient is generated within the fiber due to the low thermal conductivity of PAN-based precursors ( $\sim 0.26 \text{ W m}^{-1} \text{ K}^{-1}$ ).<sup>1,2,7,12,13</sup> The dissipation of this energy is very important and the energy generation can be controlled using slow heating rates during the thermal stabilization of the PAN-precursor fibers making this process the most time consuming step during the thermal treatment of the fibers.<sup>14,15</sup> Simultaneously, postdrawing of fibers must be performed to collapse the voids and to increase molecular orientation.<sup>8,16,17</sup> However, this orientation is partly lost due to molecular relaxation processes that occur when the PAN precursor fibers are heated up to 300°C during the stabilization step. Additional stresses must be applied during stabilization and carbonization steps in an attempt to regain the molecular orientation. This strategy results in carbon fibers with high

strength, but the limited molecular orientation prevents the fibers from developing an ultra high modulus.<sup>8,10,13</sup> There is a need for the development of novel processes that allow the acceleration of these exothermic reactions in a controlled manner to avoid fiber degradation and retain molecular orientation.

PAN-based terpolymer containing a photosensitive comonomer, such as acryloyl benzophenone, has been investigated and successfully converted into carbon fibers as reported in our prior studies.<sup>5,17</sup> In addition, polymerization and stabilization reactions are known to proceed faster and at lower temperatures when initiated by UV radiation.<sup>17–19</sup> In recent studies, on solution-cast PAN films and wet-spun PAN fibers, we established that it is possible to start cyclization and crosslinking reactions associated with thermal stabilization at lower temperatures by the external addition of a small amount (1 wt %) of photoinitiator. Subsequent UV exposure at lower temperatures led to a reduction of the conventional thermal stabilization time.<sup>20</sup> Fibers containing photoinitiator added externally into the polymer solution prior to wet-spinning (i.e., without incorporating photoinitiator into the polymer chain itself) were successfully wet spun. After further UV treatment, fibers containing photoinitiator showed higher tensile modulus and molecular orientation as compared with pure UV-treated and pure control fibers.<sup>21</sup> However, the capability of these fibers to withstand further thermal stabilization and carbonization, including accelerated heating rates, and the properties of such fibers after each thermal treatment step remain unaddressed.

Therefore, the overall goal of this research was to study the effect of the addition of photoinitiator and further UV exposure on the properties of the resulting PAN-based stabilized and carbonized fibers. The addition of photoinitiator and further UV treatment is investigated here as an alternative route to reduce the thermal stabilization processing time.

## EXPERIMENTAL

### Materials

Polyacrylonitrile homopolymer with a molecular weight ( $M_w$ ) of 233,000 and a glass transition temperature ( $T_g$ ) of 125°C was used throughout this study. This PAN homopolymer was obtained from Scientific Polymer (Ontario, NY). 4,4'-Bis(diethylamino)benzophenone (denoted as BDP) was the photoinitiator used in this study and its chemical structure is shown in Figure 1. This photoinitiator generates free radicals by hydrogen abstraction and has UV absorbance peak at 378 nm in the UVA region (320–390 nm).<sup>22–24</sup> The solvent used in this work was dimethyl sulfoxide (DMSO). Photoinitiator and solvent were obtained from Sigma-Aldrich (Aldrich Chemical Company, Mil-

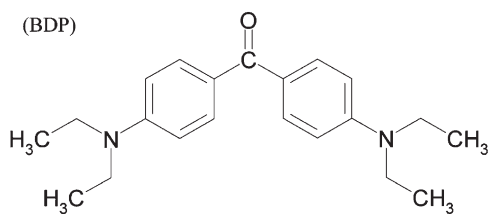


**Figure 1.** 4,4'-Bis(diethylamino)benzophenone (denoted as BDP) used throughout the study.

waukee, WI). Also, a standard silicon powder reference material was used for line position and line shape during X-ray diffraction studies (NIST reference material® 640d).

### Fiber Spinning

PAN-precursor and photoinitiator were dissolved in a 99:1 mass ratio in DMSO at 70°C. The amount of polymer in solution was kept at ~16 wt %. Fibers were spun from solution using a custom-built wet-spinning unit fitted with a spinnerette that had 100 holes nominally 68  $\mu\text{m}$  in diameter. A volumetric flow of 0.6  $\text{mL min}^{-1}$  was maintained during the spinning of the fibers. The coagulation bath consisted of 70 wt % DMSO/30 wt % distilled-deionized water. After the coagulation bath, the solidified fibers were passed through a distilled-deionized water washing bath maintained at ~20°C. The effective length of the coagulation and washing bath were 40 and 80 cm, respectively. A draw down ratio of ~1.2 was used during the wet-spinning of the PAN-based fibers. The as-spun fibers were placed in an oven and dried at 70°C for about 24 h. Next, the fibers were poststretched in a distilled-deionized water bath maintained at ~80°C. The effective length of the poststretching bath was 80 cm. A draw down ratio of ~3.0 was used during the poststretching step. Pure PAN fibers as well as fibers containing 1 wt % of photoinitiator, with an average effective diameter of ~12  $\mu\text{m}$ , were thus produced and used as the precursor fibers throughout this study.

### UV-Treatment of Fibers

The fibers were irradiated with a modified Nordson 4.5 kW UV curing lamp (Model 111465A). A mercury (Hg) arc bulb (model PM1163) was used throughout this work. Such UV sources are available commercially and used to provide a broadband output distribution in the four UV regions.<sup>19,20,25</sup> The chamber was modified to provide temperature control and the experiments reported in this study were all conducted at approximately 150°C. The intensity of this bulb was measured using a high energy UV radiometer (model PP2000, Electronic Instrumentation and Technology). Intensity values of approximately 0.228, 0.196, 0.032, and 0.095  $\text{W cm}^{-2}$  were measured for the UVA, UVB, UVC, and UVV ranges, respectively. Fiber tows approximately 10 in. long were irradiated for 300 s. The bundle of fibers was held under approximately 0.1 g denier<sup>-1</sup> of tension during the UV treatment. The distance between the samples and the UV source was kept constant at approximately 20 cm.

### Thermal Treatment of Fibers

Fiber bundles were thermally stabilized in air atmosphere using a heating rate of 2.5°C  $\text{min}^{-1}$  from 25 to 300°C, and held there for 30 min. Tension was applied to the samples during thermal oxidation by dead-weight loading. A tension of 0.1 g denier<sup>-1</sup> was applied at temperatures below 200°C, and 0.05 g denier<sup>-1</sup> above 200°C. As indicated in earlier studies, the external addition of small amounts (~1 wt %) of photoinitiator followed by a short (5 min) UV treatment increased the rate of the cyclization reaction.<sup>20,21</sup> Based on these results, UV-treated fibers with photoinitiator were placed in a preheated oven at 225°C and rapidly heated. Then, using a heating rate of 2.5°C  $\text{min}^{-1}$ , the fibers were heated to 300°C and held there for 30 min. A tension of 0.05 g denier<sup>-1</sup> was applied on these samples. Note that

the total duration of this fast-thermal stabilization step was only 60 min, which was less than half of 140 min used for the “control” thermal-only stabilization step.

Thermally stabilized fibers were then carbonized under a tension of 0.07 g denier<sup>-1</sup> in an inert environment (helium). This was accomplished by dead-weight loading using a custom-designed graphite fixture, which could be mounted inside of a graphite furnace ASTRO HP50–7010. Heating rate of 10°C min<sup>-1</sup> was used to a maximum temperature of 1200°C, and the fibers held at 1200°C for 1 h. All UV-treated and thermally stabilized and carbonized samples were compared against three types of control fibers. The first two controls consisted of only thermally stabilized pure PAN fibers and non-UV-treated fibers but containing photoinitiator. The third control consisted of fast-thermally stabilized pure PAN fibers without UV treatment. These controls were produced to confirm that the improvement in the mechanical properties and the reduction in the thermal stabilization time are due to the combined positive effect of the presence of photoinitiator and UV treatment of the samples.

### Characterization

Morphological analysis of fibers was conducted by scanning electron microscopy (SEM) with a Mitsubishi 4800 SEM unit. To retain the original cross-section shape and other physical features, the fibers were cryofractured in liquid nitrogen. To determine the effective diameter of the fibers, Image-Pro Plus 7.0 (Media Cybernetics) analysis software was used to measure the cross-section area of each type of sample. The effective diameter calculated from these area measurements is reported only as a reference. At least 40 cross-section areas were measured for each type of fiber.

A PHOENIX single filament tensile testing unit (Measurements Technology) was used to measure the mechanical properties of the different fibers types produced along this work. The single fibers were mounted on 25 mm paper tabs. At least 20 samples per type of fiber were prepared and tested.

Wide-angle X-ray diffraction (WAXD) analysis was conducted on bundles of fibers using a Rigaku-MSC (Houston, TX) X-ray diffraction unit. The X-ray source was operated at 45 kV and 0.65 mA. The X-ray diffraction pattern was captured on an image plate and the images were analyzed using Polar software v2.6.7 (Stony Brook Technology and Applied Research, STAR). The curve fitting of the spectra was done using OriginPro 7 (v7.0383, OriginLab Corporation). The unit generates a collimated X-ray beam with a wavelength of 1.5406 Å (Cu target) and a diameter of ~0.5 mm. The distances between the X-ray source and sample and the sample and the image plate detector were approximately 70 and 12 cm, respectively. Each bundle of fibers was mounted on a 10-mm paper tab and sprinkled with NIST-grade silicon standard powder for accurate allocation of 2θ position. The exposure time per sample was 2 h. Plane spacing and crystal size were calculated using the equations below:

$$\lambda = 2d \sin \theta \quad (1)$$

$$\frac{1}{d^2} = \frac{4}{3} \left( \frac{h^2 + hk + k^2}{a^2} \right) + \frac{l^2}{c^2} \quad (2)$$

$$l_a = l_c = \frac{0.89\lambda}{B \cos \theta} \quad (3)$$

$$B^2 = B_M^2 - B_S^2 \quad (4)$$

where  $\lambda$  corresponds to the wavelength of the X-ray beam,  $d$  the distance between adjacent planes in the set  $(hkl)$ ,  $\theta$  the angle of incidence of the X-ray beam, and  $a$  and  $c$  are the lattice parameters of the hexagonal crystal. Further,  $l_a$  and  $l_c$  are the crystal size,  $B$  the corrected full width at half-maximum [(full-width-at-half-max (FWHM)) intensity of the spectrum peak (on the 2θ scale), and  $B_M$  the measured FWHM.  $B_S$ , the system broadening, was determined by the silicon standard. Equation (1) corresponds to Bragg's law and eq. (2) corresponds to the lattice geometry equation for hexagonal crystal structure observed in PAN-based precursors and final carbon fibers. Equations (3) and (4) were used to calculate crystal size. Equation (3) corresponds to Scherrer formula. Warren's broadening correction, eq. (4), was used to correct the system broadening on each WAXD scan.<sup>26–34</sup> Also, conversion or aromatization indices were determined on thermally stabilized fibers using the following equation used in prior literature studies:<sup>21,29,35</sup>

$$\text{Conversion index (\%)} = \frac{A_A}{A_A + A_P} \times 100\% \quad (5)$$

where  $A_A$  is the area of the peak associated with the aromatic structure around 2θ value of 25° and  $A_P$  correspond to the area of the (1 0 0) crystal peak of PAN at 2θ = 17°. In addition, the Rigaku-MSC diffractometer is capable of measuring the orientation of the crystal in the fibers. These azimuthal intensity scans were measured for the most prominent peak of the initial PAN precursor and final carbonized fibers, which are the (1 0 0) and (0 0 2) peak, located at approximately 17° and 25°, respectively.

## RESULTS AND DISCUSSION

### Influence of UV Radiation and Photoinitiator: Thermally Stabilized Fibers

**Morphology.** Figure 2 displays representative SEM micrographs of thermally stabilized PAN fibers with and without photoinitiator. Figure 2(a,b) correspond to pure PAN fibers and those containing 1 wt % BDP, respectively. Figure 2(c,d) are representative micrographs of pure and 1 wt % BDP-PAN fibers, respectively, both UV treated. These first four specimens were conventional-thermally stabilized (140 min duration). Figure 2(e,f) correspond to pure non-UV-treated fibers and 1 wt % BDP-PAN UV-treated fibers, respectively. These two specimens were fast-thermally stabilized (60 min duration), as described in the experimental section. As observed from the micrographs, all fibers retained the characteristic kidney shape of wet-spun PAN-based fibers.<sup>3,8,28</sup> The effective diameter of pure and 1 wt % BDP PAN fibers were 9.0 ± 0.2 and 8.9 ± 0.1 μm, respectively. At 95% confidence level, there was no significant difference between the effective diameters among the different samples. In addition, no noticeable deterioration or change in the microstructure of the UV-treated fibers containing photoinitiator was observed when compared with pure control fibers. Thus, the presence of photoinitiator and further UV treatment do not significantly affect the morphology of the fibers. Another important observation is that the UV treatment of the fibers did not



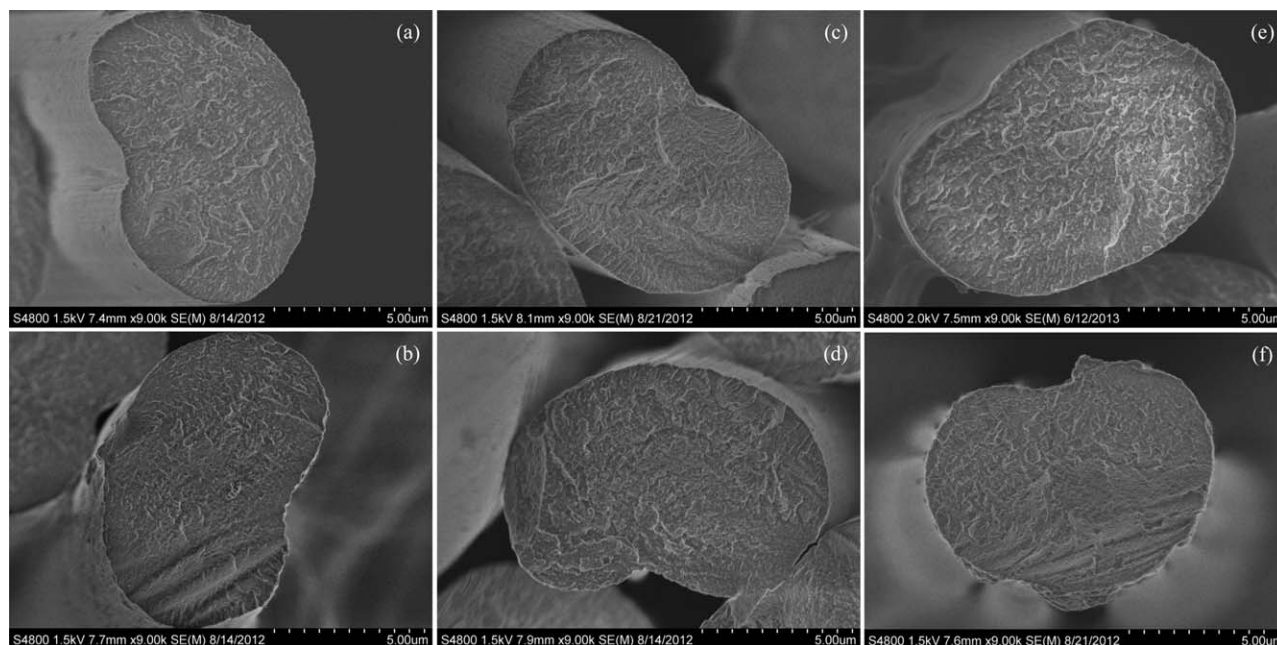


**Figure 2.** Representative SEM micrographs of thermally stabilized PAN fibers with and without photoinitiator: (a) pure PAN fibers, (b) fibers containing 1 wt % BDP, (c) pure UV-treated PAN fibers, (d) 1 wt % BDP PAN UV-treated fibers, (e) fast-thermally stabilized pure PAN fibers, and (f) fast-thermally stabilized UV-treated 1 wt % BDP PAN fibers.

lead to any obvious hollow-core structure formation in any of the UV-treated fibers. Such structure is undesired because it leads to poor quality (mechanical properties) of the stabilized and carbonized fibers.<sup>3,4,11,14,29</sup>

**Mechanical Properties.** Figure 3 displays representative tensile response of various fibers. Figure 3(a) corresponds to conventional-thermally stabilized non-UV-treated and UV-treated pure PAN fibers as well as non-UV-treated fast-thermally stabilized pure PAN fibers. Figure 3(b) is for the same treatment conditions but for fibers containing 1 wt % BDP. The limit of linear proportionality was approximately 1% for all samples.

Table I summarizes the tensile testing results conducted on single filaments. These tensile properties of the PAN fibers are consistent with those reported in the literature for experimental grade PAN fibers: 3–10% for the breaking strain, 0.1–0.5 GPa for strength, and 3–15 GPa for tensile modulus.<sup>4,5,9,13,35</sup>

Tensile properties presented in Table I indicate that there are significant differences (at 95% confidence), in the breaking strain and ultimate tensile strength between pure and 1 wt % BDP fibers. The presence of photoinitiator reduces the elongation capabilities of the non-UV-treated fibers containing photoinitiator by approximately half and the ultimate tensile strength by

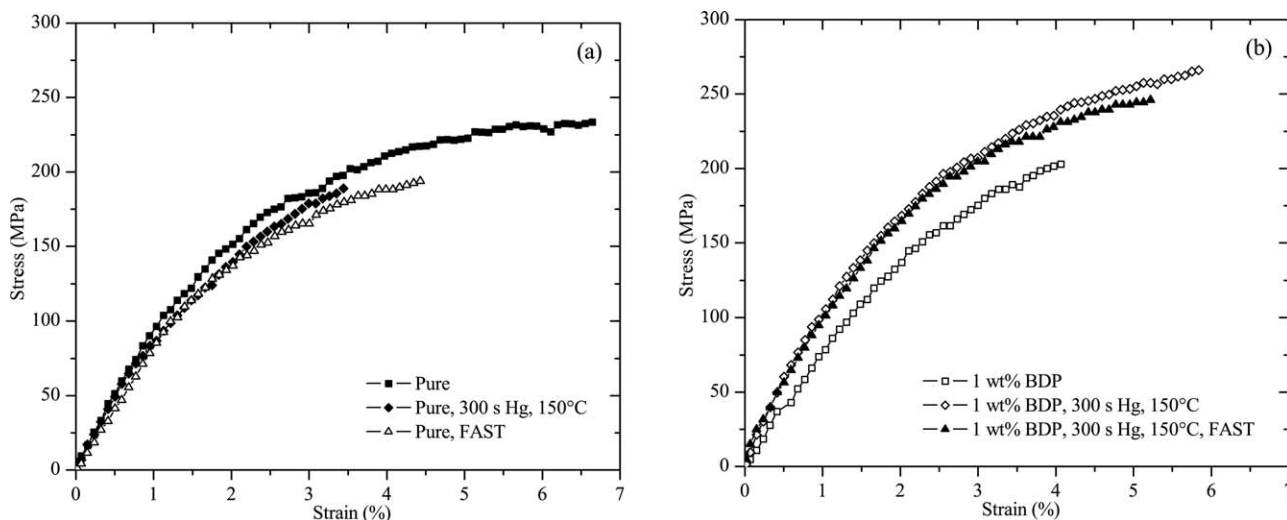


**Figure 3.** Representative tensile testing curves of each set of thermally stabilized fibers: (a) pure PAN and (b) PAN fibers containing 1% BDP.

**Table I.** Single Filament Tensile Results of Thermal Stabilized Fibers with 95% Confidence Intervals

Sample	Tensile modulus (GPa)	Max stress (GPa)	Break strain (%)
Pure	9.6 ± 0.3	0.24 ± 0.01	6.6 ± 0.8
1% BDP	9.7 ± 0.4	0.20 ± 0.02	3.7 ± 0.6
Pure, 300 s Hg, 150°C	9.6 ± 0.6	0.19 ± 0.02	3.4 ± 0.5
1% BDP, 300 s Hg, 150°C	11.2 ± 0.7	0.26 ± 0.02	5.3 ± 1.1
Pure, FAST	9.7 ± 0.3	0.19 ± 0.01	4.3 ± 0.3
1% BDP, 300 s Hg, 150°C, FAST	10.8 ± 0.5	0.25 ± 0.01	4.8 ± 0.8

~15%. These reductions could be possibly attributed to the tiny voids left by the unreacted photoinitiator during conventional thermal stabilization. Another observation was that excessive fiber fusion was observed for pure UV-treated fibers, which leads to the formation of defects on the fibers. Thus, the main phenomenon taking place during the UV treatment (at temperatures slightly above  $T_g$ ) is fiber fusion and, as shown in previous studies, polymer chain relaxation.<sup>21</sup> This leads to a significant reduction in the elongation capabilities of the fibers by approximately half and the ultimate tensile strength by ~25% between pure UV-treated and pure control fibers.

Pure fast-thermally stabilized fibers also show a significant reduction in the elongation capabilities of the fibers by approximately 35% and the ultimate tensile strength by ~25%, when compared with pure control fibers. These fast-thermally stabilized pure fibers also showed considerable fiber fusion, similar to that observed for UV-treated pure fibers. Fast heating rates during thermal stabilization led to the formation of hollow-core structure in the fibers, which is not desired because it negatively affects the mechanical properties.

Conversely, the two set of fibers containing 1 wt % BDP UV treated for 300 s (5 min) display higher tensile modulus and ultimate tensile strength than all the other set of samples (significant at 95% confidence). Specifically, conventional-thermally stabilized fibers containing 1 wt % BDP that were UV treated exhibit the highest tensile modulus and ultimate tensile strength of all six set of samples. This proves the combined positive effect of the addition of photoinitiator and 300 s of UV treatment on the fibers. The addition of photoinitiator and further UV treatment of the fibers could be used to increase the mechanical properties of the fibers during conventional thermal stabilization or reduce the thermal oxidation time (faster fiber production) while retaining the mechanical properties of the carbon fibers thus produced.

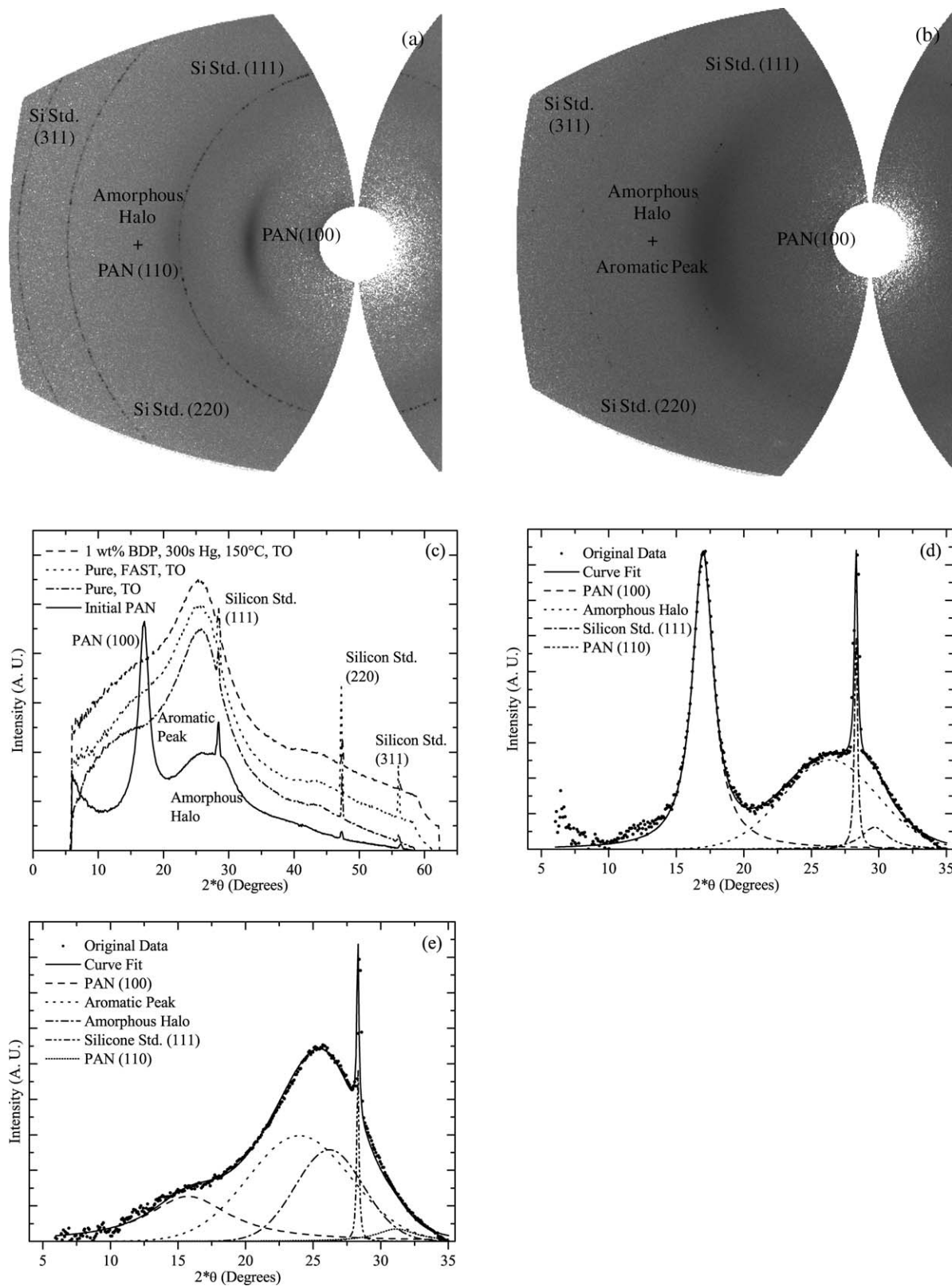
**Wide-Angle X-ray Diffraction.** Figure 4(a,b) show Fraser-corrected 2D WAXD images of poststretched and thermally oxidized PAN fibers, respectively. These images were used to obtain the integrated  $2\theta$  and azimuthal scans. Figure 4(c) shows representative  $2\theta$  scans of the most relevant set of samples: conventional-thermally stabilized UV-treated 1 wt % BDP PAN fibers, fast-thermally stabilized pure PAN fibers, conventional-thermally stabilized pure PAN fibers, and poststretched pure PAN fibers before thermal oxidation (for comparison). These  $2\theta$  scans

show the first peak at  $\sim 17^\circ$  corresponding to the (1 0 0) planes of the PAN precursor. The second peak corresponds to the combination of the amorphous halo at  $\sim 26^\circ$  and the (1 1 0) plane peak of PAN at  $\sim 29.5^\circ$ .<sup>27,28,30,36,37</sup> After the thermal stabilization step, an extra peak associated with the aromatic structure emerges at  $\sim 25^\circ$ .<sup>21,29,35</sup> Silicon standard, added to the samples for calibration purposes, shows three sharp peaks at  $28.44^\circ$ ,  $47.3^\circ$ , and  $56.12^\circ$  corresponding to its (1 1 1), (2 2 0), and (3 1 1) planes, respectively. Figure 4(d,e) display the curve fitting of  $2\theta$  scans of the poststretched and conventional-thermally oxidized PAN fibers using OriginPro software. Note that the initial location of the peaks was set to  $25^\circ$  and  $26^\circ$ , but the peak locations and widths were optimized to obtain the best curve fit.

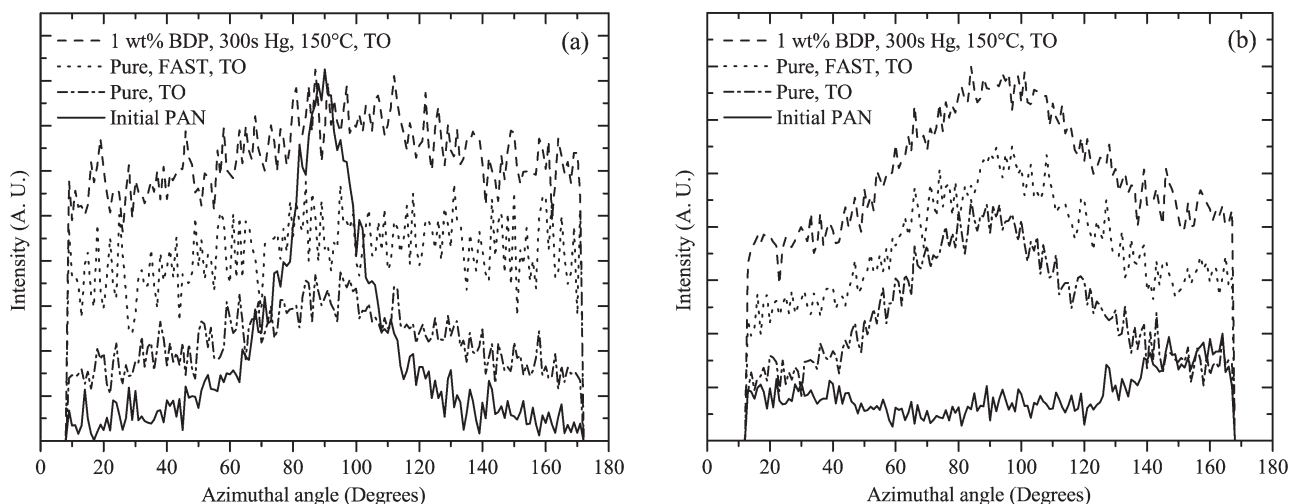
As indicated before, the crystal orientation in the fibers was measured from the azimuthal spectra of the (1 0 0) peak of the PAN and aromatic peak of the thermally oxidized fibers, as displayed in Figure 5(a,b), respectively. A sharp azimuthal peak for a given set of planes means higher orientation, whereas a broad peak indicates low orientation. As expected, due to the cyclization reaction undergone within all thermally stabilized fibers, a significant loss of orientation of the (1 0 0) peak of the initial PAN structure was observed in thermally oxidized fibers. In contrast, in Figure 5(b), the development of orientation due to the formation of the aromatic peak is observed on thermally oxidized samples. To compare the crystal orientation in the different set of fibers, the FWHM was measured for each azimuthal scan. The smaller the FWHM value, the more oriented are the crystals within the fibers.

Table II summarizes the WAXD results obtained from all the different set of samples. At 95% confidence, the interplanar spacing between the (1 0 0) planes increased and the orientation and crystal size of the original PAN structure decreased in thermally stabilized fibers when compared with initial poststretched pure PAN fibers. The conversion indices, calculated from the WAXD spectra, confirm that the conversion achieved by the samples containing 1 wt % BDP UV treated at  $150^\circ\text{C}$  for 300 s after thermal stabilization was higher than those for other sets, indicating higher cyclization of PAN. Also, these two sets of samples are able to develop a higher level of orientation of the newly formed aromatic structure.

These results agree well with the tensile testing results that show superior mechanical properties for thermally stabilized samples containing 1% BDP and UV treated for 300 s due to the fact that they are able to develop higher molecular orientation. For



**Figure 4.** Representative WAXD spectra of initial PAN and thermally oxidized (TO) PAN fibers: (a) Fraser-corrected 2D WAXD image of initial PAN fibers, (b) Fraser-corrected 2D WAXD image of conventional TO PAN fiber (c)  $2\theta$  scans obtained with Polar software, (d) Post-stretched PAN WAXD curve fitting using OriginPro, and (e) TO PAN WAXD curve fitting using OriginPro.



**Figure 5.** Representative azimuthal WAXD spectra of poststretched PAN and thermally oxidized (TO) PAN fibers: (a) Azimuthal scans of the PAN (1 0 0) peak, (b) Azimuthal scans of the developing aromatic peak.

this system, higher molecular orientation leads to higher mechanical properties of the fibers.<sup>7,10,13,16</sup> It is noted that the duration of the thermal stabilization step for some of the UV-treated samples containing photoinitiator was less than half the thermal stabilization time used for the control fibers. In addition, this novel UV-induced stabilization step was conducted at a lower temperature than the ones used during conventional thermal oxidation process, which are between 200 and 300°C.<sup>2,5,8,13,14,17</sup> These results establish the potential of the current results for developing a more rapid process for stabilization of PAN-based precursors to produce carbon fibers more efficiently.

In contrast, fast-thermally stabilized pure control fibers show higher level of degradation of the initial PAN structure, which is shown by the larger FWHM of the (1 0 0) peak and lower conversion index and orientation of the aromatic structure. Note that in a previous study, it was demonstrated that during the thermal stabilization of PAN using the same amount of tension, the orientation of the PAN polymer chains decreases, that is, larger FWHM of the (1 0 0) peak was observed as the conversion index increases.<sup>21</sup> All these results indicate that fast thermal stabilization of PAN precursors leads to excessive degradation of the PAN precursor, formation of hollow-core structure within the fibers, and reduction of the mechanical properties of the fibers.

**Influence of UV Radiation and Photoinitiator: Carbon Fibers Morphology.** Figure 6 displays representative SEM micrographs of carbonized PAN fibers with and without photoinitiator. Figure 6(a,b) correspond to carbon fibers obtained from pure PAN fibers and those containing 1 wt % BDP, respectively. Figure 6(c,d) are representative micrographs of carbon fibers obtained from UV-treated pure and 1 wt % BDP-PAN fibers, respectively. These first four specimens were conventional-thermally stabilized. In contrast, Figure 6(e,f) correspond to carbon fibers from fast-thermally stabilized non-UV-treated pure and UV-treated 1 wt % BDP-PAN fibers, respectively. In all cases, carbon fibers retained the characteristic kidney shape of wet-spun PAN-based fibers.<sup>3,8,28</sup> The effective diameter of pure and 1 wt % BDP PAN fibers were  $6.6 \pm 0.1$  and  $6.4 \pm 0.1$   $\mu\text{m}$ , respectively. There was no significant difference between the effective diameters among the different samples.

No noticeable deterioration or change in the microstructure was observed for UV-treated fibers containing photoinitiator when compared with pure control fibers. Thus, the presence of photoinitiator and UV treatment did not significantly affect the morphology of the fibers. Another important observation is that the UV treatment of the fibers did not lead to any obvious hollow-core structure formation. However, this is not the case for fast-thermally stabilized pure fibers. SEM micrographs, Figure 7,

**Table II.** WAXD Results of Thermally Oxidized Fibers and Initial Poststretched Fibers (For Comparison) with 95% Confidence Intervals

Sample	$a$ ( $\text{\AA}$ )	$l_a$ ( $\text{\AA}$ )	(1 0 0) FWHM ( $^\circ$ )	Aromatic Peak FWHM ( $^\circ$ )	C. I. (%)
Initial Pure (before thermal stabilization)	$6.001 \pm 0.020$	$42.3 \pm 1.9$	$26.1 \pm 0.9$	N/A	N/A
Pure	$6.438 \pm 0.049$	$10.5 \pm 0.9$	$100.4 \pm 2.1$	$71.2 \pm 1.9$	$70.4 \pm 2.4$
1% BDP	$6.470 \pm 0.026$	$9.7 \pm 0.7$	$106.1 \pm 3.7$	$71.6 \pm 1.9$	$68.2 \pm 1.5$
Pure, 300 s Hg, 150°C	$6.471 \pm 0.048$	$10.4 \pm 0.5$	$105.6 \pm 3.3$	$70.9 \pm 2.9$	$70.5 \pm 1.4$
1% BDP, 300 s Hg, 150°C	$6.557 \pm 0.042$	$10.6 \pm 0.6$	$129.7 \pm 3.7$	$63.9 \pm 2.2$	$78.9 \pm 3.7$
Pure, FAST	$6.521 \pm 0.046$	$9.8 \pm 0.7$	$163.4 \pm 5.8$	$77.8 \pm 1.6$	$65.2 \pm 1.5$
1% BDP, 300 s Hg, 150°C, FAST	$6.502 \pm 0.058$	$10.6 \pm 1.1$	$124.5 \pm 2.8$	$64.4 \pm 1.7$	$77.0 \pm 1.6$



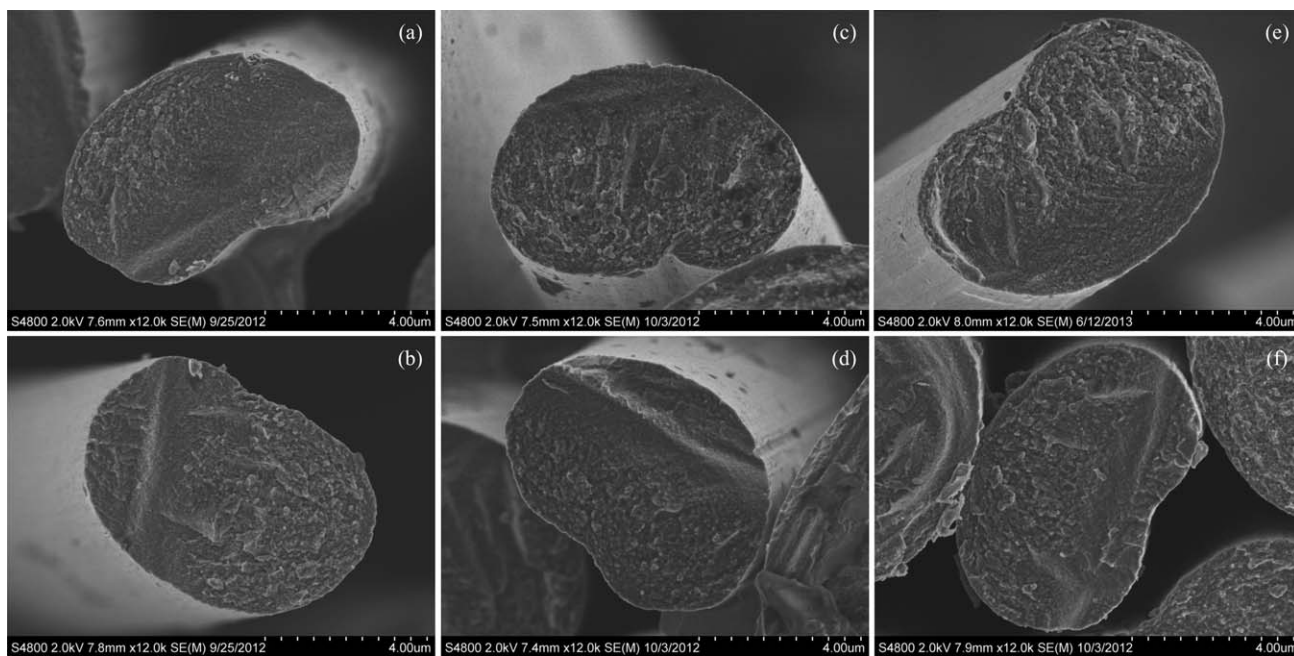


**Figure 6.** Representative SEM micrographs of carbonized PAN fibers with and without photoinitiator: (a) pure PAN fibers, (b) fibers containing 1 wt % BDP, (c) pure UV-treated PAN fibers, (d) 1 wt % BDP PAN UV-treated fibers, (e) fast-thermally stabilized pure PAN fibers, and (f) fast-thermally stabilized UV-treated 1 wt % BDP PAN fibers.

clearly shows hollow-core defects observed in fast-thermally stabilized pure PAN carbon fibers attributed to inadequate thermal stabilization. Figure 7(a,b) display a hollow-core fiber and fused hollow fibers, respectively. Note that these defects were not observed in any other set of samples. As discussed in the following section, such defects lead to lower mechanical properties of the fibers.<sup>4,11,14,29</sup>

**Mechanical Properties.** Figure 8 displays representative tensile response of various carbonized fibers. Figure 8(a) corresponds to carbon fibers obtained from conventional-thermally stabilized non-UV-treated pure and UV-treated pure as well as fast-thermally stabilized pure PAN fibers. Figure 8(b) shows the same treatment conditions but for fibers containing 1 wt % BDP, and Table III summarizes all of the tensile results. These tensile properties of carbon fibers are consistent with those reported in the literature for commercial and experimental grade PAN-based carbon fibers: 0.3–2.5% for the breaking strain, 0.1–6.5 GPa for strength, and 30–500 GPa for tensile modulus.<sup>4,5,8,13,38,39</sup>

Tensile testing results shown in Table III indicate that there are significant differences in the breaking strain and ultimate tensile strength between carbon fibers obtained from pure control and pure UV-treated fibers. The UV treatment reduces the elongation capabilities of the pure fibers and the ultimate tensile strength by approximately 33%. These reductions may be attributed to the fiber surface defects resulting from excessive fiber fusion observed on pure UV-treated fibers. As mentioned before, it is believed that the main phenomena taking place during the UV treatment (at temperatures slightly above the  $T_g$  of the PAN precursor without photoinitiator) are fiber fusion and polymer chain relaxation, which lead to a significant reduction

in the elongation capabilities and ultimate tensile strength of the fibers.

Carbon fibers produced from pure fast-thermally stabilized fibers also show a significant reduction in the tensile modulus of the fibers by  $\sim 10\%$  and the ultimate tensile strength by  $\sim 20\%$  (at 95% confidence) when compared with “pure” control counterparts. For these specimens, considerable fiber fusion is observed as well, similar to the one observed on pure UV-treated fibers. Fast heating rates during thermal stabilization lead to the formation of hollow-core fibers (Figure 7), which is not desired because it negatively affects the mechanical properties of the fibers, as confirmed by the tensile results.

For carbon fibers obtained from UV-treated fibers containing photoinitiator, the results are significantly different: the two set of fibers containing 1 wt % BDP UV treated for 300 s (5 min) display higher tensile modulus and ultimate tensile strength than all the other set of samples. Specifically, carbon fibers obtained from conventional-thermally stabilized UV-treated fibers containing 1 wt % BDP exhibit the highest tensile modulus of all six set of samples (significant at 95% confidence). An improvement in the tensile modulus of approximately 20% was observed in carbon fibers obtained from conventional-thermally stabilized UV-treated fibers containing 1 wt % BDP when compared with conventional-thermally stabilized control pure PAN fibers.

Carbon fibers obtained from UV-treated fast-thermally stabilized fibers containing 1 wt % BDP exhibit higher tensile modulus and ultimate tensile strength when compared with conventional and fast-thermally stabilized pure fibers. UV-treated fast-thermally stabilized fibers containing 1 wt % BDP show around 10, 15, and 25% improvement in the tensile modulus when compared with conventional-thermally stabilized



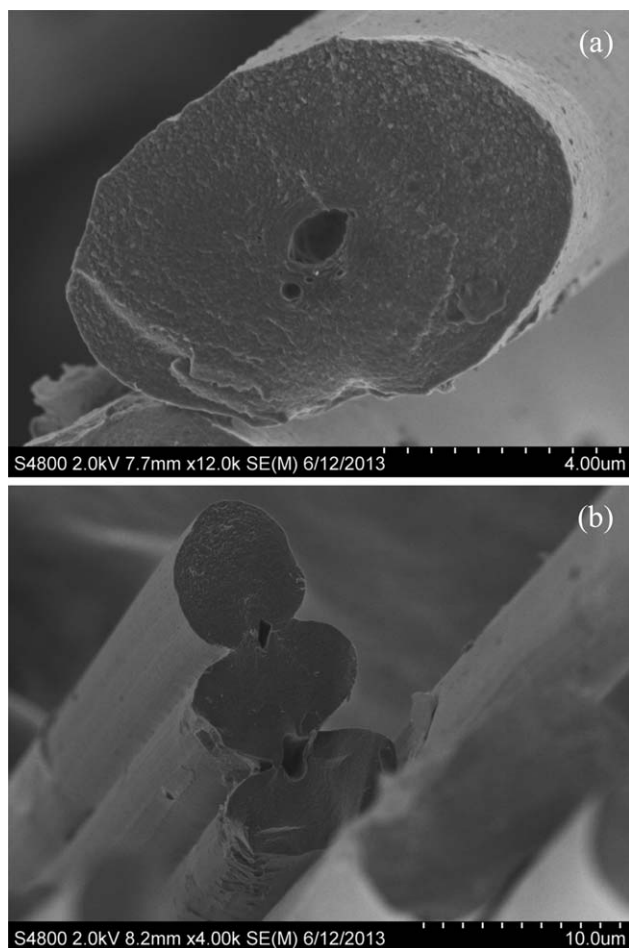


**Figure 7.** SEM micrographs of defects observed on fast-thermally stabilized pure PAN carbon fibers attributed to inadequate thermal stabilization: (a) hollow-core fiber, (b) fused hollow fibers.

pure, non-UV treated conventional-thermally stabilized 1 wt % BDP fibers, and fast-thermally stabilized pure control fibers, respectively. In addition, carbon fibers obtained from UV treated fast-thermally stabilized fibers containing 1 wt % BDP

display approximately 33% improvement in the ultimate tensile strength when compared with fast-thermally stabilized pure control fibers. It is important to note that, besides the demonstrated improvement in the mechanical properties, the fast-thermal stabilization step takes less than half the duration of the conventional thermal stabilization (60 vs. 140 min, respectively). This proves the combined positive effect of the addition of photoinitiator and 300 s of UV treatment on the precursor fibers. The addition of photoinitiator and further UV treatment of the fibers could be used to increase the mechanical properties of the fiber during conventional thermal stabilization or reduce the thermal oxidation time (faster fiber production) while retaining the mechanical properties of the carbon fibers thus produced.

**Wide-Angle X-ray Diffraction.** Figure 9(a) shows an illustrative Fraser-corrected 2D WAXD image of the PAN-based carbon fibers. Figure 9(b) shows representative  $2\theta$  scans of the most relevant set of carbonized samples: conventional-thermally stabilized UV-treated 1 wt % BDP PAN fibers, fast-thermally stabilized pure PAN fibers, and conventional-thermally stabilized pure PAN fibers. These integrated  $2\theta$  scans, displayed in Figure 9(b), show the first peak at  $\sim 25^\circ$  corresponding to the (0 0 2) plane of the turbostratic structure of PAN-based carbon fibers. The second peak at  $\sim 42^\circ$  corresponds to the (1 0 0) plane.<sup>32–34,40</sup> As mentioned earlier, NIST-grade silicon standard was added to all fiber samples for accurate  $2\theta$  measurements. Figure 9(c) illustrates curve-fitting of the  $2\theta$  peak associated with (0 0 2) planes of carbon fibers and (1 1 1) peak associated with the silicon standard.

The orientation of the crystals in the fibers was measured from the azimuthal scans conducted on the (0 0 2) peak, which is the most prominent peak of the carbon fiber WAXD spectra. Figure 9(d) shows the azimuthal scans of the (0 0 2) peak. To compare the crystal orientation in the different set of fibers, the FWHM was measured for each azimuthal scan. The smaller the FWHM value, the more oriented are the crystals within the fibers.

Table IV summarizes the WAXD results obtained from all samples. At 95% confidence, fast-thermally stabilized pure carbon

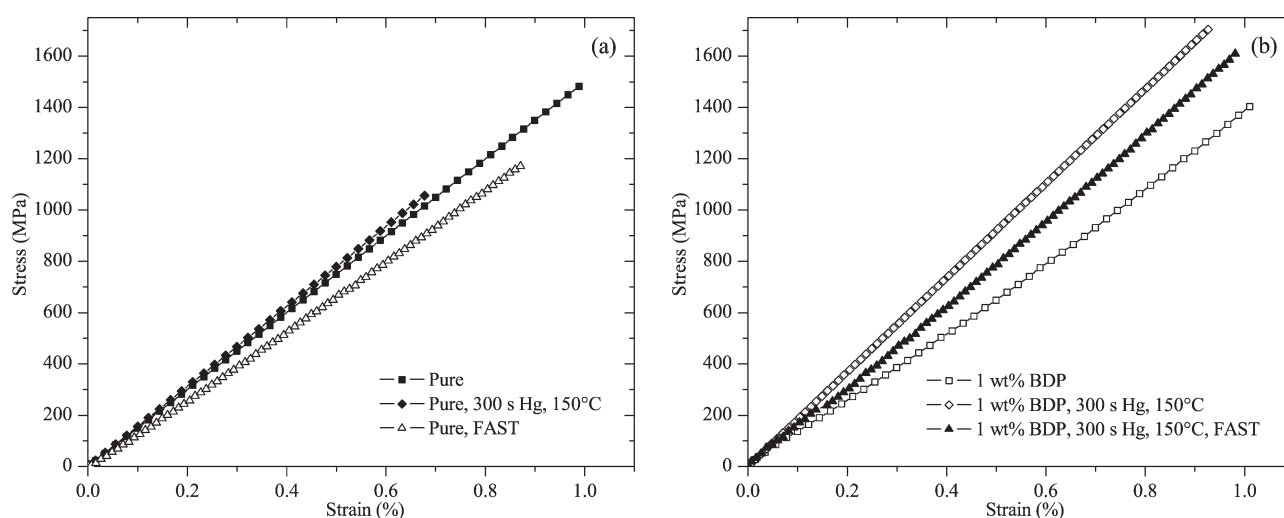


**Figure 8.** Representative tensile testing curves of each set of carbonized fibers derived from: (a) pure PAN, (b) PAN fibers containing 1 wt % BDP.

**Table III.** Single Filament Tensile Properties of Carbon Fibers (Error Bars Indicate 95% Confidence Intervals)

Sample	Tensile modulus (GPa)	Max stress (GPa)	Break strain (%)
Pure	153.5 ± 6.6	1.47 ± 0.17	1.0 ± 0.1
1% BDP	150.2 ± 10.1	1.40 ± 0.20	0.9 ± 0.1
Pure, 300 s Hg, 150°C	157.6 ± 6.2	1.05 ± 0.13	0.7 ± 0.1
1% BDP, 300 s Hg, 150°C	184.8 ± 10.4	1.65 ± 0.12	0.9 ± 0.1
Pure, FAST	137.9 ± 4.8	1.22 ± 0.18	0.9 ± 0.1
1% BDP, 300 s Hg, 150°C, FAST	170.6 ± 6.0	1.60 ± 0.11	1.0 ± 0.1

fibers show smaller crystal size values and level of orientation as compared with conventional-thermally stabilized control pure carbon fibers. These results are consistent with the lower mechanical properties and hollow-core defects observed on this set of fibers. These results indicate that fast-thermal stabilization of pure PAN precursors leads to excessive degradation of the PAN precursor, formation of hollow-core structure within the

fibers, loss of orientation, smaller crystal size, and reduction of the mechanical properties of the fibers.

This is not the case for carbonized UV-treated fibers containing photoinitiator. The results shown in Table IV indicate no negative effects for the (0 0 2) *d*-spacing and size of the crystals for carbon fibers obtained from UV-treated PAN fibers containing photoinitiator as compared with all other types of carbon fibers.

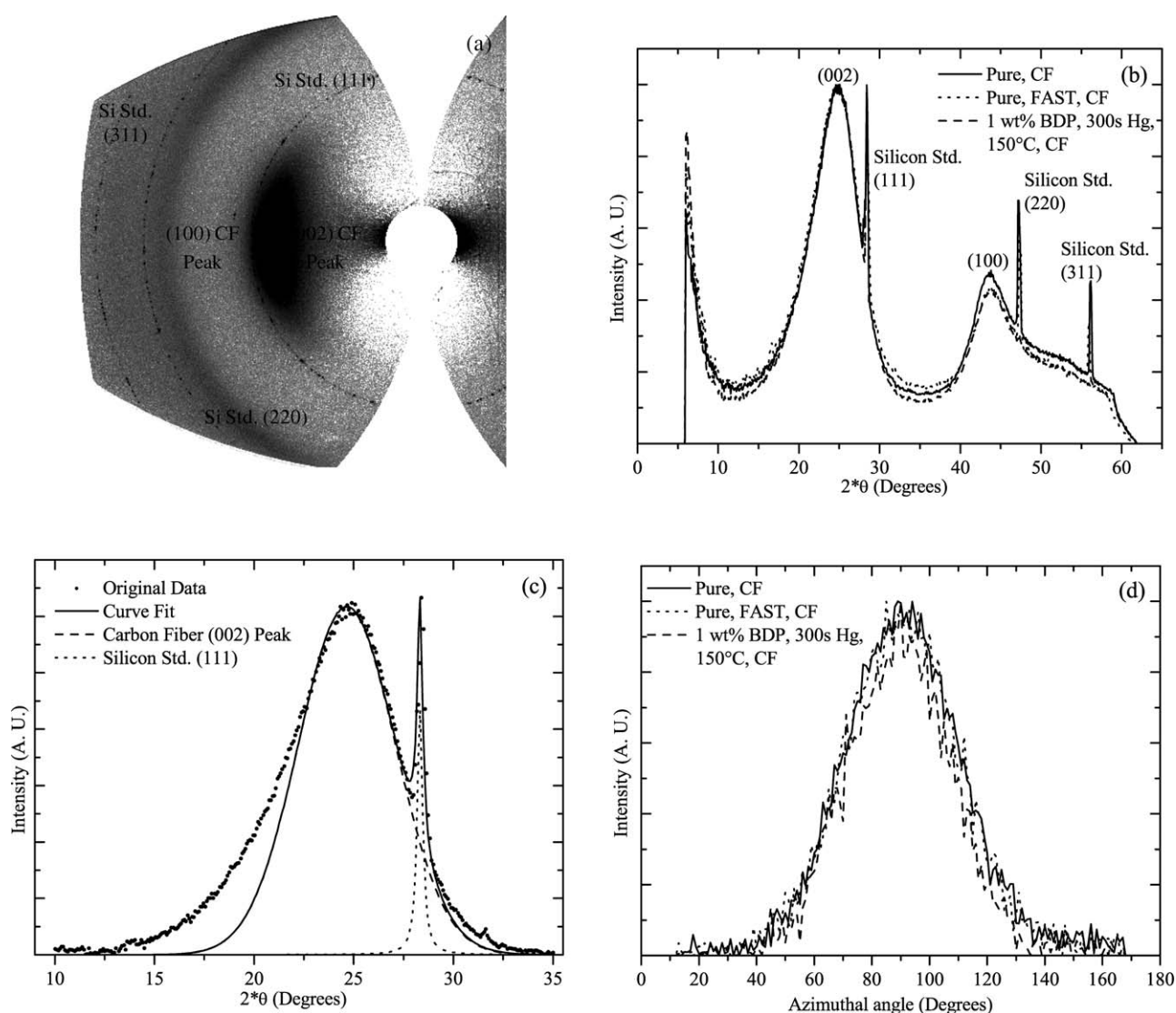


**Figure 9.** Representative WAXD spectra of the produced Carbon Fibers (CF): (a) Fraser-corrected 2D WAXD image (b)  $2\theta$  scans obtained with Polar software, (c) PAN CF WAXD curve fitting using OriginPro, and (d) azimuthal scans of the (0 0 2) peak.

**Table IV.** WAXD Results of Carbon Fibers with 95% Confidence Intervals

Sample	$l_c$ (Å)	(0 0 2) $d$ -spacing (Å)	(0 0 2) FWHM (°)
Pure	14.4 ± 0.2	3.586 ± 0.004	45.4 ± 0.7
1% BDP	14.1 ± 0.3	3.585 ± 0.007	45.4 ± 0.8
Pure, 300 s Hg, 150°C	14.0 ± 0.6	3.586 ± 0.011	46.1 ± 0.8
1% BDP, 300 s Hg, 150°C	14.0 ± 0.2	3.575 ± 0.011	43.4 ± 0.7
Pure, FAST	13.4 ± 0.3	3.597 ± 0.009	46.1 ± 0.6
1% BDP, 300 s Hg, 150°C, FAST	14.4 ± 0.5	3.580 ± 0.008	44.2 ± 0.3

Also these two sets of samples are able to develop a higher level of orientation when compared with the other groups of carbon fibers.

These results agree well with the tensile testing results that show superior mechanical properties for carbonized fibers derived from PAN containing 1% BDP and UV treated for 300 s due to the fact that they are able to develop higher molecular orientation. For this system, higher molecular orientation leads to higher mechanical properties of the fibers.<sup>7,8,10,13,16</sup> These results prove the combined positive effect of the addition of photoinitiator and 300 s of UV treatment on the fibers prior thermal stabilization. At the same thermal treatment conditions, it was possible to enhance the mechanical properties of the final carbon fibers by the addition of photoinitiator and subsequent UV treatment. In addition, with this novel process, it was possible to reduce the thermal stabilization time by more than half keeping the final mechanical and physical properties of the produced carbon fibers. These results may be used in the development of a novel and more rapid process for stabilization of PAN-based precursors to produce carbon fibers more efficiently.

## CONCLUSIONS

A rapid, dual-stabilization route for the production of carbon fibers from PAN-based precursor fibers was successfully demonstrated. Photoinitiator, 4,4'-bis(diethylamino)benzophenone, was effectively added to PAN solution before the fiber wet-spinning step to UV-induced crosslinking and cyclization reactions at a lower temperature in the produced PAN-based fibers. After UV treatment, precursor fibers could be rapidly thermally stabilized and successfully carbonized. SEM micrographs show no obvious deterioration of the microstructure or presence of hollow-core in the UV-treated fibers containing photoinitiator after thermal stabilization and carbonization. In contrast, fast-thermally stabilized pure PAN carbon fibers show hollow-core fiber defects attributed to inadequate thermal stabilization.

Tensile testing results confirm that fibers containing 1 wt % photoinitiator that were UV treated display higher tensile modulus and ultimate tensile strength than other sets not subjected to that treatment. Pure UV-treated and fast-thermally stabilized pure PAN fibers display a reduction in their mechanical properties when compared with pure slow-thermally stabilized control fibers. These reductions were attributed to the loss of molecular orientation and excessive fiber fusion leading to defect formation. WAXD results confirm that the fast-thermal stabilization of pure PAN precursors leads to excessive degradation of the PAN precursor, loss of orienta-

tion, and smaller crystal size in the fibers. In contrast, no negative effects were observed on the (0 0 2)  $d$ -spacing and size of the crystals within the UV-treated fibers containing photoinitiator. In summary, these results establish the positive effect of the addition of photoinitiator and UV treatment in reducing the thermal stabilization time by more than half while maintaining the final mechanical and physical properties of the carbon fibers.

## ACKNOWLEDGMENTS

As a subcontractor to Cytec Carbon Fibers, LLC under AFRL Prime Contract No.FA8650-05-D-5807 (AFRL/RXBT Program Monitor: Dr. Karla Strong), Clemson University received partial financial assistance to support the initial phase of this overall project, which is gratefully acknowledged.

## REFERENCES

- Catta Preta, I. F.; Sakata, S. K.; Garcia, G.; Zimmermann, J. P.; Galembeck, E.; Giovedi, C. *J. Therm. Anal. Calorim.* **2007**, *87*, 657.
- Zhang, W.; Li, M. *J. Mater. Sci. Technol.* **2005**, *21*, 581.
- Sedghi, A.; Farsani, R. E.; Shokuhfar, A. *J. Mater. Process Technol.* **2008**, *198*, 60.
- Jie, L.; Wangxi, Z. *J. Appl. Polym. Sci.* **2005**, *97*, 2047.
- Mukundan, T.; Bhanu, V. A.; Wiles, K. B.; Johnson, H.; Bortner, M.; Baird, D. G.; Naskar, A. K.; Ogale, A. A.; Edie, D. D.; McGrath, J. E. *Polymer* **2006**, *47*, 4163.
- Reisch, M. S. *Chem. Eng. News* **2011**, *89*, 10.
- Gupta, A. K.; Paliwal, D. K.; Bajaj, P. *J. Macromol. Sci.: Rev. Macromol. Chem. Phys.* **1991**, *C31*, 1.
- Edie, D. D.; Diefendorf, R. J. In *Carbon-Carbon Materials and Composites*; Buckley, J. D.; Edie, D. D., Eds.; National Aeronautics and Space Administration: Washington, DC, **1992**, pp 19–39.
- Shiedlin, A.; Marom, G.; Zilkha, A. *Polymer* **1985**, *26*, 447.
- Wu, G.; Lu, C.; Ling, L.; Hao, A.; He, F. *J. Appl. Polym. Sci.* **2005**, *96*, 1029.
- Hou, Y.; Sun, T.; Wang, H.; Wu, D. *J. Appl. Polym. Sci.* **2008**, *108*, 3990.
- Hou, J.; Wang, X.; Zhang, L. *Appl. Phys. Lett.* **2006**, *89*, 152504–1.
- Paiva, M. C.; Kotasthane, P.; Edie, D. D.; Ogale, A. A. *Carbon* **2003**, *41*, 1399.
- Hou, Y.; Sun, T.; Wang, H.; Wu, D. *Text Res. J.* **2008**, *78*, 806.



15. Mittal, J.; Bahl, O. P.; Mathur, R. B. *Carbon* **1997**, *35*, 1196.
16. Tan, L.; Pan, J.; Wan, A. *Colloid. Polym. Sci.* **2012**, *290*, 289.
17. Naskar, A. K.; Walker, R. A.; Proulx, S.; Edie, D. D.; Ogale, A. A. *Carbon* **2005**, *43*, 1065.
18. Decker, C. In *Photochemistry and Polymeric System*; Kelly, J. M.; Mc Ardle, C. B.; Maunder, M. J. de F., Eds.; Royal Society of Chemistry: Cambridge, **1993**, pp 32–46.
19. Endruweit, A.; Johnson, M. S.; Long, A. C. *Polym. Compos.* **2006**, *27*, 119.
20. Morales, M. S.; Ogale, A. A. *J. Appl. Polym. Sci.* **2013**, *128*, 2081.
21. Morales, M. S.; Ogale, A. A. *J. Appl. Polym. Sci.* **2013**, *130*, 2494.
22. Ledwith A. In *Photochemistry and Polymeric Systems*, Kelly, J. M.; Mc Ardle, C. B.; Maunder, M. J. de F., Eds.; Royal Society of Chemistry: Cambridge, **1993**, pp 1–14.
23. Fouassier, J. P. *Prog. Org. Coat.* **1990**, *18*, 229.
24. Kubota, H.; Ogiwara, Y. *J. Appl. Polym. Sci.* **1982**, *27*, 2683.
25. Boyd, I. W.; Zhang, J. Y. *Nucl. Instrum. Methods Phys. Res Sect. B* **1997**, *121*, 349.
26. Cullity, B. D. *Elements of X-Ray Diffraction*; Addison-Wesley Publishing Company: Reading, **1978**.
27. Dong, X.; Wang, C.; Juan, C. *Polym. Bull.* **2007**, *58*, 1005.
28. Dong, X.; Wang, C.; Bai, Y.; Cao, W. *J. Appl. Polym. Sci.* **2007**, *105*, 1221.
29. Yu, M.; Wang, C.; Bai, Y.; Wang, Y.; Xu, Y. *Polym. Bull.* **2006**, *57*, 757.
30. Bashir, Z. *J. Macromol. Sci.: Phys.* **2001**, *40 B*, 41.
31. Hu, X.-P. *J. Appl. Polym. Sci.* **1996**, *62*, 1925.
32. Iwashita, N.; Park, C. R.; Fujimoto, H.; Shiraishi, M.; Inagaki, M. *Carbon* **2004**, *42*, 701.
33. Short, M. A.; Walker, P. L., *J. Carbon* **1963**, *1*, 3.
34. Gupta, A.; Harrison, I. R.; Lahijani, J. *J. Appl. Crystallogr.* **1994**, *27*, 627.
35. Ko, T.; Ting, H.; Lin, C. *J. Appl. Polym. Sci.* **1988**, *35*, 631.
36. Yu, M.; Wang, C.; Bai, Y.; Zhu, B.; Ji, M.; Xu, Y. *J. Polym. Sci. Part B* **2008**, *46*, 759.
37. Matta, V. K.; Mathur, R. B.; Bahl, O. P.; Nagpal, K. C. *Carbon* **1990**, *28*, 241.
38. Katzman, H. A.; Adam, P. M.; Le, T. D.; Hemminger, C. S. *Carbon* **1994**, *32*, 379.
39. Wang, P. H.; Yue, Z. R.; Li, R. Y.; Liu, J. *J. Appl. Polym. Sci.* **1995**, *56*, 289.
40. Warren, B. E.; Bodenstein, P. *Acta Crystallogr.* **1966**, *20*, 602.